

Preparation and dielectric properties of highly preferred-(100) orientation (Pb, La)(Zr, Ti)O₃ antiferroelectric thick films by sol–gel processing

Xiujian Chou · Maoxiang Guo · Yating Zhang · Jun Liu · Wendong Zhang

Received: 2 July 2011 / Accepted: 13 September 2011 / Published online: 22 September 2011
© Springer Science+Business Media, LLC 2011

Abstract Pb_{0.97}La_{0.02}Zr_{0.95}Ti_{0.05}O₃ (PLZT) antiferroelectric thick films of highly preferred-(100) orientation with different thickness were successfully deposited on Pt(111)/Ti/SiO₂/Si(100) substrates depending on the sol–gel process technique. The effects of the PLZT thick films in the preparation and electric properties are investigated. The films show polycrystalline perovskite structure with a (100) preferred orientation by X-ray diffractometer analyses. The antiferroelectric nature of the thick films is demonstrated by P (polarization)–E (electric field). The temperature dependence of the dielectric constant and dielectric loss displays the similar behavior in both cases at 100 kHz while the values of polarization characteristic are decreased with the increase of the film thickness. The phase switching current are studied as a function of a gradually change dc electric field and the voltage dependent current density of the most highly (100)-oriented PLZT film is 1.49×10^{-8} A/cm² over electric field range from 0 to ± 261 kV/cm. The film at 2,498 nm exhibits excellent dielectric properties and highly preferred-(100) orientation.

Keywords Antiferroelectric thick films · Different thickness · Sol–gel process · Dielectric properties · Highly preferred-(100)-orientation

1 Introduction

Lead zirconate (PbZrO₃) of perovskite structure was the primal compound identified as an antiferroelectric in 1950s [1]. Because of their unique properties and different electric-field inducted phase, such as under dc electric field, antiferroelectric materials have remarkable change of polarization, strains and current during the AFE-FE switching, the Pb-based antiferroelectric ceramics as well as thick films, for example, (Pb, La)(Zr, Ti)O₃ (PLZT) [2], Pb(Zr, Sn, Ti)O₃ (PZST) [3] and Pb(Nb, Zr, Sn, Ti)O₃ (PNZST) [4] would be researched extensively in energy storage, high-strain transducers/actuators and pyroelectric thermal sensors. (Pb, La)(Zr, Ti)O₃ antiferroelectric materials have high potential utility for devices in microelectronic applications due to their unique dielectric, piezoelectric and electro-optical properties. Nowadays, along with the fast development of the fabrication technology, PLZT materials show highly potential for microelectromechanical systems (MEMS) [5].

PLZT thick films could be deposited through various methods, such as metallorganic chemical vapour deposition MOCVD [6], sol–gel [7], sputtering [8], pulsed laser deposition PLD [9] and so on. Sol–gel technique is the convenient and low cost method. Particularly due to the molecular lever of all of the starting chemicals in the solution, the composition of the multicomponent system is easily controlled and a high degree of homogeneity of the thick films of antiferroelectric can be expected. Therefore, the most antiferroelectric films for heterogenous integration are prepared by sol–gel processing.

In this paper, (Pb, La)(Zr, Ti) O₃ thick films of different thickness were deposited on Pt(111)/Ti/SiO₂/Si(100) substrates by sol–gel process. The combination of antiferroelectric thick films with silicon micromachining technology laid a good foundation for further study in microactuators.

X. Chou (✉) · M. Guo · Y. Zhang · J. Liu · W. Zhang
Key Laboratory of Instrumentation Science and Dynamic
Measurement, North University of China, Ministry of Education,
Taiyuan, China
e-mail: chouxujian@nuc.edu.cn

The dielectric properties of PLZT antiferroelectric thick films with different thickness including phase switching strains, the temperature-dependent characteristics and so on were studied systematically.

2 Experimental detail

The $\text{Pb}_{0.97}\text{La}_{0.02}(\text{Zr}_{0.95}\text{Ti}_{0.05})\text{O}_3$ antiferroelectric thick films were processed by sol-gel deposition process from Fig. 1 showing. Raw materials were lead acetate trihydrate [$\text{Pb}(\text{CH}_3\text{COO})_2 \cdot 3\text{H}_2\text{O}$], lanthanum acetate [$\text{La}(\text{CH}_3\text{COO})_3$], zirconium propoxide [$\text{Zr}(\text{OC}_3\text{H}_7)_4$], and titanium isopropoxide [$\text{Ti}[\text{OCH}(\text{CH}_3)_2]_4$]. Acetate was chosen as a solvent. At the beginning of step, on the basis of the predetermined number, lead acetate trihydrate with 15% excess, lanthanum acetate hydrate, and acetic acid were mixed in a ratio. The solution was distilled at 110 °C for 1 h in order to clear up water. Following pulsing titanium isopropoxide and zirconium propoxide into the above the solution and would be mixed for 30 min until the above mixed solution was cooled to room temperature. Distilled water was put into the proportion of 20 mol of distilled water to 1 mol of lead during the mixing process as so to stabilize the solution. However, because this solution which was produced was not very stable, the solution became gel after a few days. For removing this phenomenon and making the solution stable better, needed adding lactic acid as the function of catalyzer and chelation into the solution in the proportion of 1 mol of lactic acid to 1 mol of lead. To improve the mechanical properties of the gel film as researching of the properties of Antiferroelectric PLZT, ethylene glycol was mixed into the solution in the proportion of 1 mol of ethylene glycol to 1 mole of lead. Finally, in order to gain the solution about 0.4 mol/L the solution, there must be added into acetic acid and 2-methoxyethanol. The goal of addition of 2-methoxyethanol was that the 2-methoxythano could improve the wetability and lower the surface tension of the solution.

PLZT thick films, leaved 24 h, were also fabricated on the substrates of Pt(100)/Ti/SiO₂/Si(100) by spin-coating method. Each PLZT layer was spin coated at 5,000 rpm for 20 s, in order to get the best properties of the $\text{Pb}_{0.97}\text{La}_{0.02}(\text{Zr}_{0.95}\text{Ti}_{0.05})\text{O}_3$, there must be adapted two temperature of pyrolyzed which one was 30 °C for 10 min, the other was 600 °C for 10 min, to heat treatment. Then the spin coatings were repeated several times to obtain desired thickness. In order to prevent the losing of a large of lead in the film when the film was processing anneal at hyperther, a capping layer of 0.4 mol/L PbO precursor solution will be prepared from lead acetate trihydrate, was added in the end before the film went through a final anneal at 700 °C for 30 min to produce the perovskite phase. Finally, several film samples (sample A, B and C) with

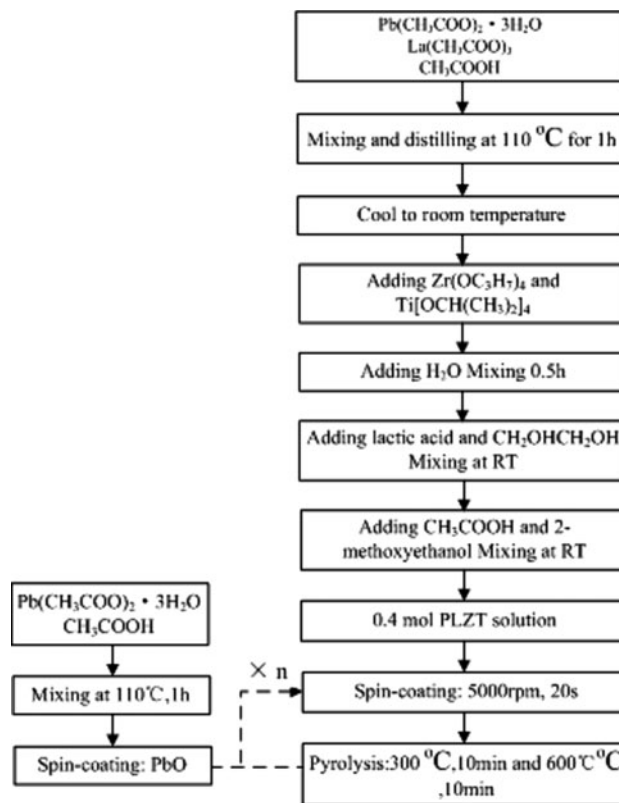


Fig. 1 Flow diagram of sol-gel processing for PLZT thick films

thickness between 1 and 4 μm had been posed. Gold pads of 0.5 mm in diameter were covered on the film surface as top electrodes by dc sputtering.

The crystal orientation of PLZT thick films is researched by X-ray diffractometer (XRD). And the microstructures of PLZT thick films are examined by the atomic force microscope (AFM). The leakage current–electric field characteristic of the PLZT antiferroelectric thick films is examined at room temperature by a Keithley 6517A electrometer. The field-induced hysteresis loops of the PLZT thick films are demonstrated by a modified Sawyer–Tower circuit. The temperature and field dependence dielectric constant and dielectric loss are obtained using an Agilent 4284A LCR meter.

3 Results and discussion

Cross-section SEM images for PLZT thick films with different thickness are shown in Fig. 2. It can be seen that all the films have smooth and uniform thickness and the thicknesses of the PLZT thick films are 1,215, 2,498 and 3,817 nm at sample A, B and C, respectively. The average thickness of one coating layer is 0.12 μm.

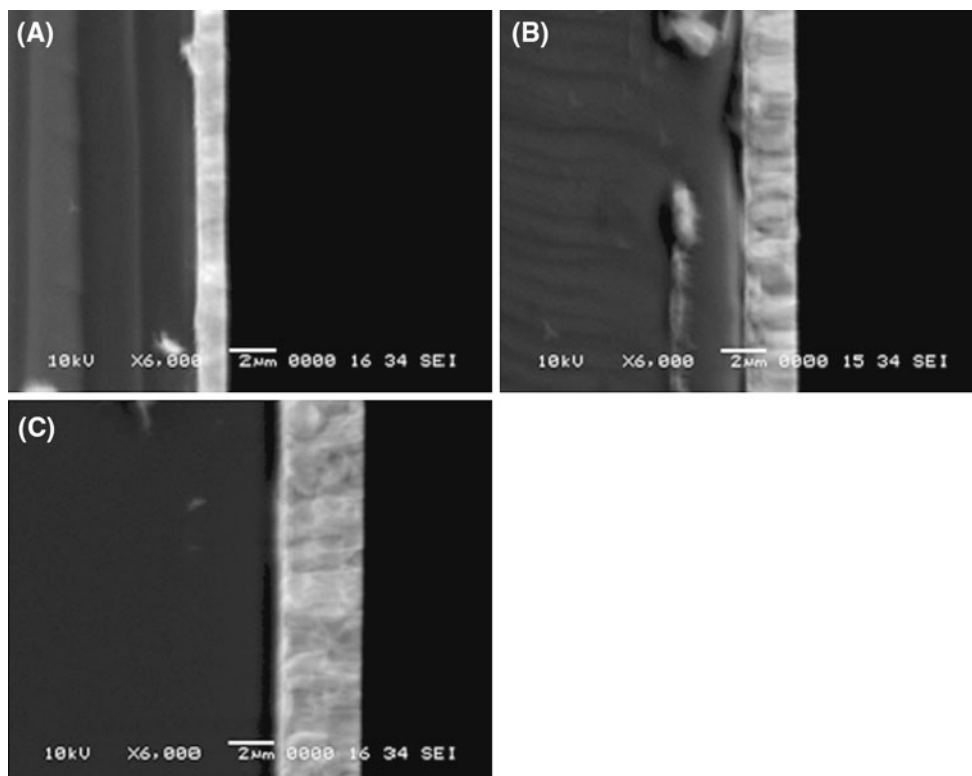


Fig. 2 Cross-section SEM images for PLZT thick films with different thickness

The surface morphology of the PLZT thick films with different thickness are analyzed through scanning electron microscopy (SEM). Figure 3 expresses a typical film microstructure, free of cracks and having fairly homogeneous morphology. As can we have known from Fig. 3 that the film is smooth, dense, and uniform with average grain sizes of about 522, 630, and 829 nm at sample A, B and C, respectively, which suggest that the grain sizes and the density of the film grow with the increasing of film thickness. The distributing of grain sizes of sample B is the more uniform and homogeneous than others. However, the film of sample B is the ones with the highest crystallinity. It can be seen, those characteristics are highly important for the application of PLZT as electrooptic material.

Using the Software which name is The Image post-processing software of 4.5, we can get the data of the average grain size and roughness. They would be determined from surface analyses though AFM are seen in Table 1 and in Fig. 4 which illustrate the influence of thickness on grain size and roughness. It can be seen that the sample B is better smooth on surface than others, because of the uniform for the distributing of grain sizes lead to have the smallest roughness [10].

The X-ray diffraction patterns of the PLZT antiferroelectric thick films are given in Fig. 5 and are recorded with a step of $0.02^\circ/\text{min}$ within the 2θ range from 20 to

60°C . It can be seen that all the film are a pure polycrystalline perovskite structure with (100), (111), (110), (200) and present a higher (100) orientation. The (100)-preferred orientation of the film is formed by the presence of (001)-oriented PbO buffer layer. The (001)-oriented PbO crystals on the surface of the platinum electrode provide nucleation sites for the overlaid PLZT films and enhance the formation of their (100) orientation [11]. In order to research the effect of different thickness of the PLZT thick films on the (100) orientation, we use the following formula to calculate the orientation factor of (100),

$$\text{Orientation factor}(F) = \frac{I(100)}{[I(100) + I(110) + I(111)]} \quad (1)$$

According to the Eq. 1 [12], the (100)-orientation factor for films at sample A, B and C were 0.10, 0.73 and 0.57, respectively. Obviously, The PLZT thick film of sample B shows more highly preferred-(100) orientation (at $2\theta = 22^\circ$, Fig. 5) than others. Higher (100)-preferred orientation implies that the nucleation of the PLZT films are weakly controlled by the substrate effect [13]. Considering the distributing of grain sizes at different thickness, an uniform and cracked of grain sizes matching with the films and the substrates may lead to enhance (100)-preferred orientation in the films.

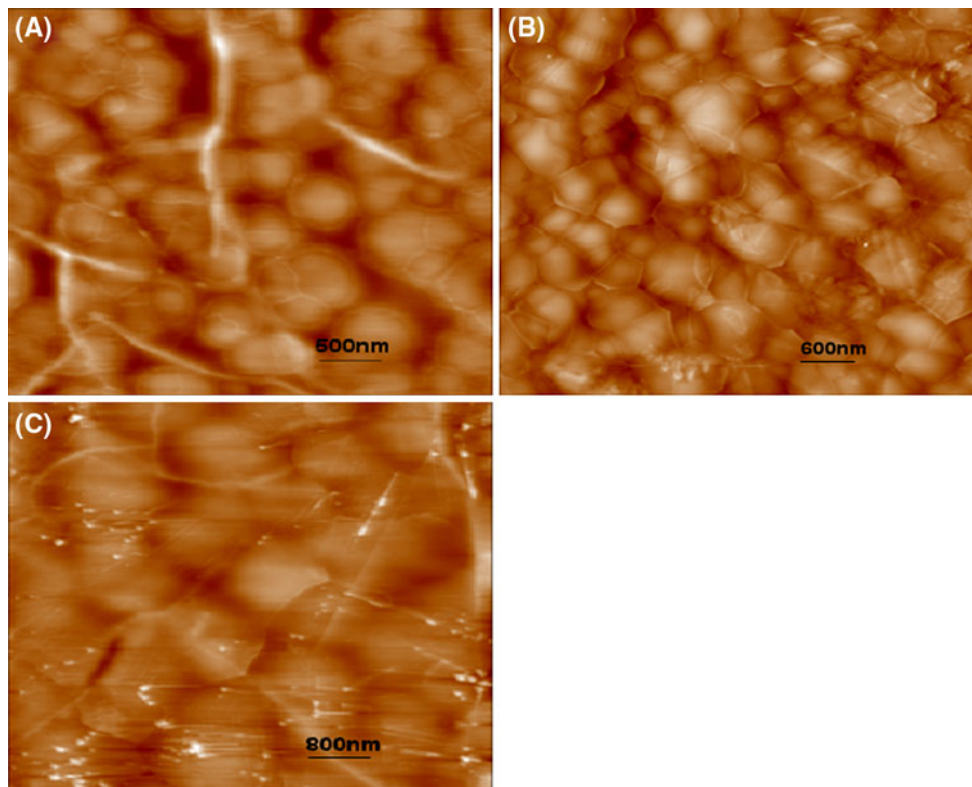


Fig. 3 AFM images of PLZT antiferroelectric thick films at different thickness

In order to research the effects of which properties of PLZT film, Hysteresis loops (P–E) of PLZT thick films are measured in Fig. 6 at room temperature and 100 kHz. As well known that PLZT thick films clearly show the double hysteresis loops under the action of the applied electric field. It is better presented the AFE nature of the PLZT films with respective thicknesses and translated into the ferroelectric phase in electric field. According to increase of the electric field, the polarization shows a gradual adding and decreasing, and it also indicates a diffused phase switching between AFE and FE Phases. The double hysteresis loops also demonstrate that the field dependant phase of the films of “slanted” is gradually changing, and it is also gradually completing between the antiferroelectric and the ferroelectric phase. According as the Fig. 6, the values of maximum polarization of the PLZT thick films of sample A, B and C are 38, 43 and 45 $\mu\text{C}/\text{cm}^2$, respectively. Then

Table 1 Variation of grain size and roughness in function of different thickness

Thickness (nm)	Roughness (nm)	Average grain size (nm)
1,215	6.41	522
2,498	6.24	630
3,817	6.77	829

the hysteresis loops go through a change from the slanted to the square form with the addition of thickness content for samples. As clearly seen that, with the increasing of thickness of PLZT film, the maximum polarization of the film is enhancing. The forward (AFE-FE) phase switching field and backward (FE-AFE) phase switching field are 70, 205 kV/cm, 74, 211 kV/cm and 82, 223 kV/cm for sample A, B and C, respectively. Obviously, AFE-FE (E_F) and FE-AFE (E_A) phase switching fields is gradually increasing with the increase of thickness of film. This can be attributed to the higher film thickness [14]. And also this difference is attributed to the crystalline orientation. Meanwhile, unlike antiferroelectric ceramic blocks (the residual polarization are zero). A small amount of remnant polarization (P_r) in the samples which are due to the leakage and the influence of stress of substrates, are decreasing with increasing thickness. The increasing of P_{max} and the reducing P_r may be result from combinative effects of (100)-preferred orientation and grain sizes [13].

Figure 7 shows the dielectric constant and dielectric loss of PLZT thick films at sample A, B and C, respectively, as a function of temperature under the frequency 100 kHz. It can be seen that following the increasing of temperature, the dielectric constant and the dielectric losses also can increase until getting the Curie temperature which are 221, 220, and 215 $^{\circ}\text{C}$, respectively, and it can influence the

Fig. 4 3D-AFM result of PLZT thick films of different thickness

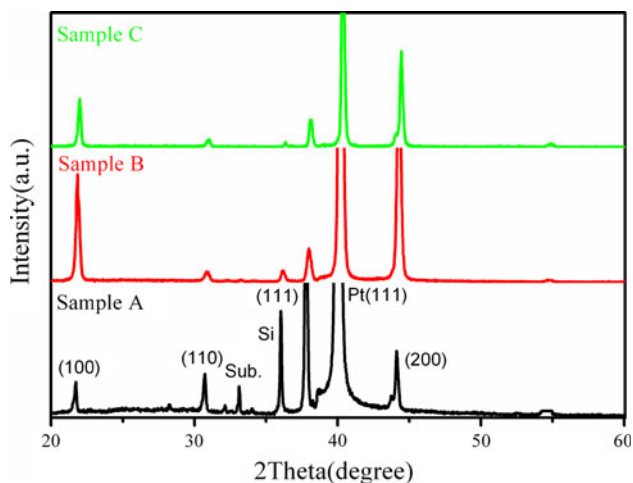
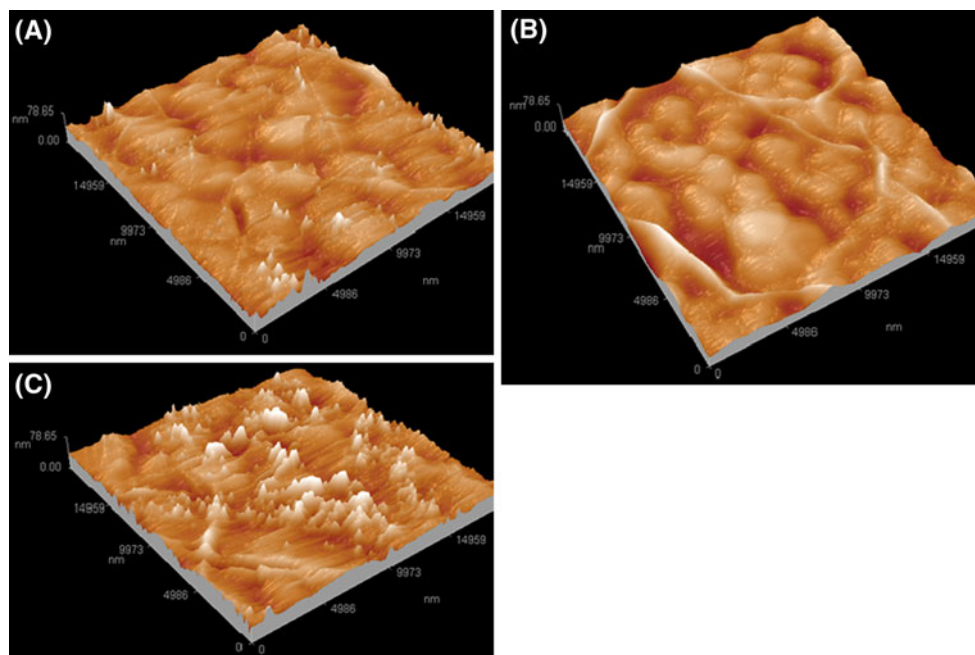


Fig. 5 XRD patterns of PLZT thick films of different thickness grown on the Pt(111)/Ti/SiO₂/Si substrate

stability of antiferroelectric. It leads to happen tiny shift of the Curie temperature. Then the dielectric constant and the dielectric losses are gradually reducing due to the phase transformation of AFE-to-PE, and the temperature will continue to increase. As greatly seen from Fig. 6 that the PLZT film of sample B have higher dielectric constant and lower dielectric loss at the low frequency (less than 100 kHz) contrast to sample A and C owing to enhancing the (100)-preferred orientation and the grain sizes of film.

In order to observe the change of current owing to transforming phase, the current density–field (J – E) curves of different thickness of PLZT thick films are measured in Fig. 8. The electric field is worked following the measurement mode is from 0 to $+E_{max}$, then $+E_{max}$

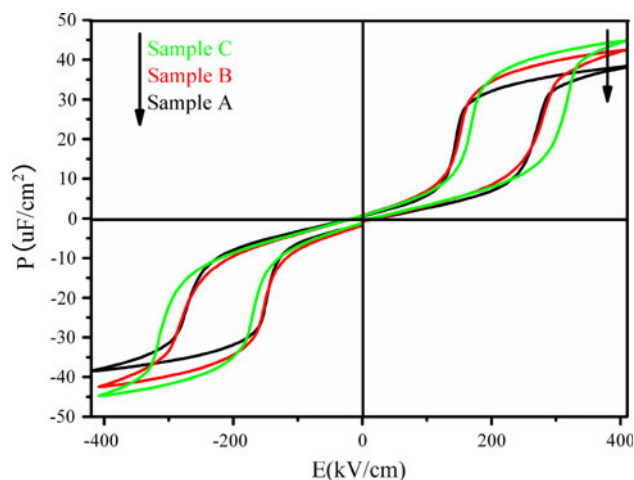


Fig. 6 The hysteresis loops of PLZT antiferroelectric thick films at different thickness

to $-E_{max}$ and $-E_{max}$ to 0, which is stepped with a time lag of 1 s. As well known, the leakage current (denoted as I_l) and the induced current (denoted as I_p) make up of the overall current (denoted as I) that result from the AFE-FE phase transformation or the FE-to-AFE phase transformation. During polarization and depolarization, the leakage current and current are caused by turn of dipole. Owing to having the high quality of the film in all samples, the leakage current is very small, compared with the current causing by polarization and depolarization in the measurement range. It is shown from the Fig. 8 that the leakage current and induced current are both produced during the AFE-FE phase transformation or the FE-AFE phase transformation, however, the maximum current can be

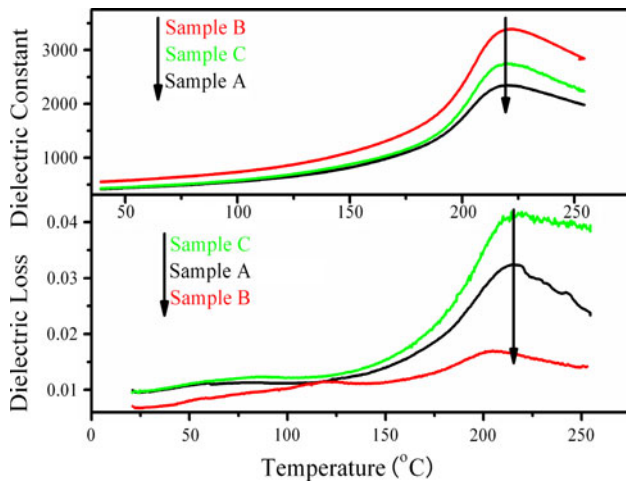


Fig. 7 Temperature dependence of the dielectric constant and dielectric loss of the PLZT thick films at different thickness

appeared, because the same direction with the leakage current and induced current cause and the induced current is more than leakage current by phase switching from AEF to FE. The maximum current density are $4.4 \times 10^{-9} \text{ A/cm}^2$ at 170 kV/cm^2 , $1.49 \times 10^{-8} \text{ A/cm}^2$ at 180 kV/cm^2 and $5.2 \times 10^{-9} \text{ A/cm}^2$ at 176 kV/cm^2 at sample A, B and C, respectively. The differences in the maximum current density have connection with the amount of the polarized unit area and the phase switching procedure of the film. On the contrary, during the phase switching from FE to AFE, the maximum reverse current would be caused due to the reason that is the opposite direction with the leakage current and the induced current. It also can be found from the maximum current density that the induced current is gradually decreasing in the phase switching and the properties of PLZT is gradually decreasing. At the same time, the phase transition current is higher than the leakage current. Hence, under the FE-to-AFE phase transformation, the measured current is negative and has a smaller value in contrast to the current density gained from the AFE-FE process. The film of sample B has the best steady than others, because of having the maximum current density in the FE-to-AFE phase transformation.

4 Conclusion

$\text{Pb}_{0.97}\text{La}_{0.02}\text{Zr}_{0.95}\text{Ti}_{0.05}\text{O}_3$ (PLZT) antiferroelectric thick films at different thickness are fabricated on Pt(111)/Ti/SiO₂/Si(100) substrates by sol–gel process. The film of sample B, whose orientation factor is 0.73, has the higher preferred-(100) orientation (at $2\theta = 22^\circ$) and better grain sizes than sample A and C. The hysteresis loops are changed from slanted to square, and the maximum polarization are 38, 43 and $45 \mu\text{C/cm}^2$ at sample A, B and C,

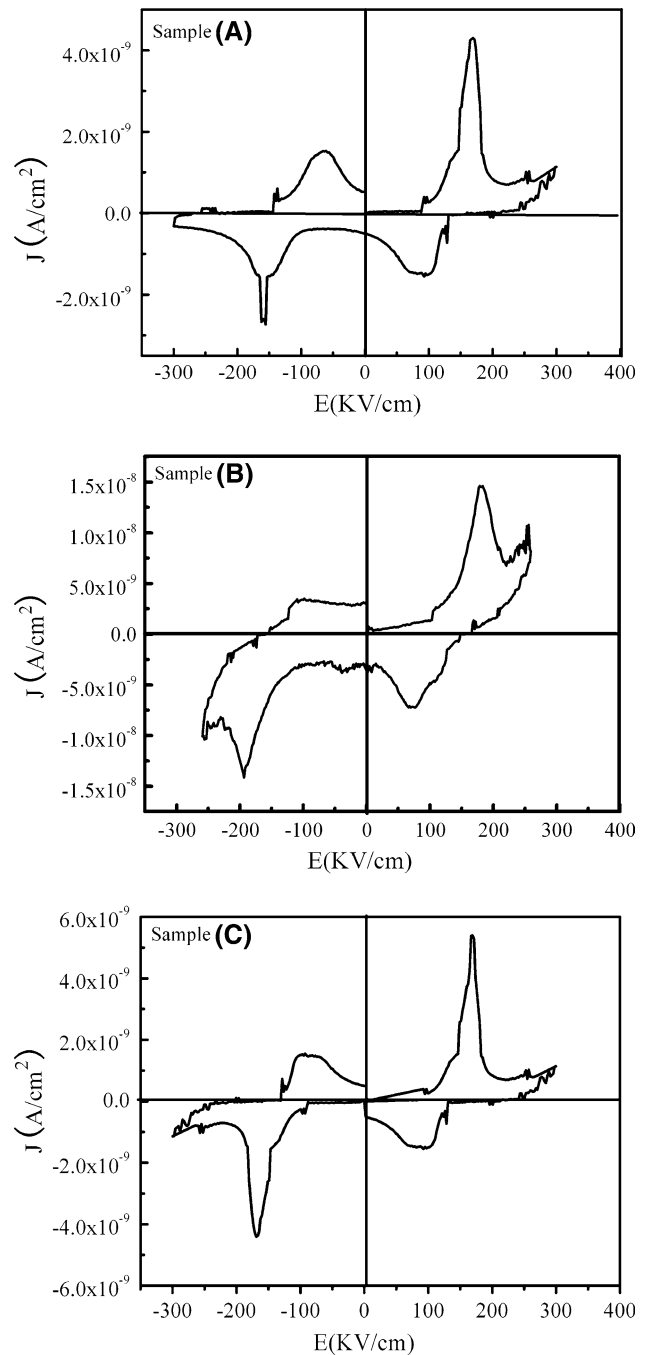


Fig. 8 Phase switching current of the PLZT thick films of different thickness

respectively. The dielectric constant of the sample B is higher than others, but the dielectric loss is the lowest. The Curie temperature of the film at different thickness are 221, 220, and $215 \text{ }^\circ\text{C}$, respectively. The J–E curves explained that the maximum current density are $4.4 \times 10^{-9} \text{ A/cm}^2$ at 170 kV/cm^2 , $1.49 \times 10^{-8} \text{ A/cm}^2$ at 180 kV/cm^2 and $5.2 \times 10^{-9} \text{ A/cm}^2$ at 176 kV/cm^2 for the PLZT film at sample A, B and C in the phase transformation,

respectively. The PLZT thick film of sample B has the best steady. In conclusion, the PLZT thick films of 2,498 nm have the best electric property of all, which are helpful for the application of these films in MEMS devices.

Acknowledgment The authors would like to acknowledge the support from the National Natural Science Foundation of China under Grant No. 60806039 and No. 51175483, Shanxi Provincial Natural Science Foundation of China under Grant No. 20100210023-6, and supported by Shanxi Provincial Young Leaders on Science.

References

1. Shirane G, Sawaguchi S, Takagi Y (1951) *Ibid* 84:476
2. Kong LB, Ma J (2002) *Mater Lett* 56:30
3. Yang P, Payne DA (1992) *J Appl Phys* 71:1361
4. Zhai J, Cheung MH, Xu ZK, Li X, Chen H, Colla EV, Wu TB (2002) *J Appl Phys Lett* 81:3621
5. Bharadwaja SSN, Krupanidhi SB (2000) *Mater Sci Eng B* 78:1–10
6. Kojima T, Sakai T, Watanabe T, Funakubo H, Saito K, Osada M (2002) *Appl Phys Lett* 80:2746
7. Zhengkui Xu, Wai-Hung Chan (2007) *Acta Mater* 55(11):3923–3928
8. Bharadwaja SSN, Krupanidhi SB (2000) *J Appl Phys* 88(4):2072–2080
9. Yingbang Yao, Jiwei Zhai, Haydn Chen (2004) *J Appl Phys* 95(11):6341–6346
10. Simoes AZ, Gonzalez AHM, Zaghete MA, Varela JA, Stojanovic BD (2001) Effects of annealing on the crystallization, roughness of PLZT thin films. *Thin Solid Films* 384:132–137
11. Wen G, Li JF, Chu XC, Gui ZL, Li LT (2004) Preparation and characterization of sol-gel derived (100)-textured $\text{Pb}(\text{Zr}, \text{Ti})\text{O}_3$ thin films: PbO seeding role in the formation of preferential orientation. *Acta Mater* 52:2787–2793
12. Yu J, Meng XJ, Sun JL et al (2004) *J Appl Phys* 96:2792
13. Zhang SQ, Wang LD, Li WL, Li N, Fei WD (2011) Effects of lanthanum doping on the preferred orientation, phase structure and electrical properties of sol-gel derived $\text{Pb}_{1-3x/2}\text{Lax}(\text{Zr}_{0.6}\text{Ti}_{0.4})\text{O}_3$ thin films. *J Alloys Compd* 509(6):2976–2980
14. Zhengkui X, Chan W-H (2007) Preparation and electrical properties of highly (111) oriented antiferroelectric PLZST films by radio frequency magnetron sputtering. *Acta Mater* 55:3923–3928